



## Bivariate Splines over Triangular Meshes for Freeform Surface Modeling with Sharp Features

Juan Cao[ORCID]<sup>1</sup> and Jianmin Zheng[ORCID]<sup>2</sup>

<sup>1</sup>Xiamen University, China, [Juancao@xmu.edu.cn](mailto:Juancao@xmu.edu.cn)

<sup>2</sup>Nanyang Technological University, Singapore, [asjmzheng@ntu.edu.sg](mailto:asjmzheng@ntu.edu.sg)

### ABSTRACT

This paper presents a novel scheme for constructing bivariate spline surfaces over triangular meshes which are topologically equivalent to a disk. The core part of the scheme is a set of knot selection rules that define local configurations of a triangulation called the directed-one-ring-cycle (D1RC) configurations and bivariate splines defined over a D1RC configuration that are new non-tensor-product splines and possess many nice properties of a univariate B-spline. Using D1RC splines, we take an input triangular mesh as a control mesh and define a bivariate spline surface from the control mesh, which mimics the standard NURBS modeling. Moreover, we can introduce sharp features into the overall smooth spline surface by simply setting special D1RC configurations. As a result, the proposed scheme can define spline surfaces in a way similar to that of NURBS, but has less restriction on the connectivity of the input control mesh.

**Keywords:** surface modeling, bivariate splines, triangular meshes, sharp features.

### 1 INTRODUCTION

Generalizing univariate B-splines to bivariate splines is a basic strategy to construct spline surfaces in freeform surface modeling. A popular approach is to use tensor-product. A typical example is NURBS which has been an industry standard in CAD/CAE [17]. NURBS has many good properties such as clear geometric intuition, compact representation, automatic maintenance of smoothness, analytic formula, local control, and many nice algorithms. However, due to inherent tensor-product structure, NURBS has two serious limitations: (1) NURBS does not support local refinement which is often demanded in interactive modeling and engineering simulation; and (2) NURBS has difficulty in modeling shapes of arbitrary topology. To solve the first limitation, T-splines were proposed [19,20], which allow the existence of T-junctions in the control grid of the surface definition and thus enable local refinement. To solve the second limitation, subdivision surfaces were developed [4,10,21], which generalize B-spline surfaces to arbitrary topology. Due to the nature of recursive subdivision process, subdivision surfaces are not so widely used in CAD/CAE as in animation and game industry.

Another approach to generalizing univariate B-splines to bivariate splines is by non-tensor product methods, examples of which include surfaces over triangular domains [1,11,14], Box-splines [8], and simplex splines [7]. In particular, Box-splines are defined over uniform grids and are still constrained by the connectivity of the grids. Simplex splines are more general than Box-splines. A well-known

simplex spline is the triangular B-spline or DMS-spline [6,13,18], which has similar setup as B-splines but needs to explicitly add auxiliary knots.

The recent generalization of univariate B-splines is bivariate splines over the so-called “Delaunay configurations” (DCB-splines) [15,16]. DCB-splines and univariate B-splines share many useful properties such as the smoothness and polynomial reproduction. They are considered to be the very promising multivariate generalization of univariate B-splines and have been successfully used in data reconstruction and visualization [3,2,9,5]. Despite their mathematical elegance, the DCB-splines do not provide an ideal user-interface for interactive modeling. In particular, the connectivity relation among the control points of a DCB-spline is ambiguous. As a result, it is not easy to determine which region of the surface will be influenced when one or some control points are manipulated. Moreover, the number of bases is unknown before the actual computation of Delaunay configuration.

In this paper, we present a novel scheme to construct bivariate spline surfaces from triangular meshes which are topologically equivalent to a disk. Triangular meshes are nowadays widely used in geometric modeling. Thus our work can be compatible with existing modeling systems. The key technique behind the scheme is a set of new knot selection rules that define local configurations of a triangulation, which we call the directed-one-ring-cycle (D1RC) configurations. The D1RC configurations of a triangulation are used to define bivariate splines. Based on the concept of D1RC configurations, we define a bivariate spline surface from the input triangular mesh, which is piecewise rational. We call such surfaces D1RC-spline surfaces. The advantages of the D1RC-spline surfaces are that they define the surfaces in a similar fashion of standard NURBS, i.e., the input meshes serve as the control meshes which give a rough approximation of the surfaces; there is no need to add auxiliary knots; and the resulting surfaces are  $C^{k-1}$  continuous for degree  $k$  surfaces. Moreover, shape features can also be modeled by simply setting special D1RC configurations. Overall, the contributions of the paper are three-folds:

- We define D1RC configurations on an arbitrary triangulation domain, which are used for knot selection. Based on the D1RC configurations, we further define D1RC-spline functions that share many nice properties as univariate B-splines.
- We present a novel approach to define a rational spline surface from an input triangular mesh. The surface has nice geometric properties as NURBS, which include affine invariance, local control, convex hull properties,  $C^{k-1}$  continuity where  $k$  is the degree of the surface, etc.
- We also provide a strategy to create sharp features in an overall smooth surface intuitively.

The rest of the paper is organized as follows. Section 2 introduces some concepts and notations that will be used in the paper. Section 3 presents a knot selection method so that we can define a bivariate spline space over a 2D triangulation. Section 4 describes how to define a bivariate spline surface from an input 3D triangular mesh such that the triangular mesh serves as a control grid and how to introduce sharp features into the bivariate spline surface. Section 5 gives a few examples to demonstrate the modeling using the proposed bivariate spline surface scheme. Section 6 concludes the paper.

## 2 PRELIMINARIES

For a set of two dimensional points  $V = \{v_i \mid i = 1, \dots, n\}$ , its triangulation is denoted by  $T = \{V, E, F\}$  where  $E = \{e_j \mid e_j = (v_{j_1}, v_{j_2})\}$  and  $F = \{f_k \mid f_k = (v_{k_1}, v_{k_2}, v_{k_3})\}$  are a set of edges and faces. A vertex, an edge or a face is called an element of triangulation  $T$ . In the context of splines, 2D vertices used for defining splines are often called “knots”. So in the paper we use the terms “vertex” and “knot” without distinction when there is no ambiguity. For a triangulation  $T$ , if  $A$  is a set of vertices of an element of  $T$ ,  $\Gamma^f(A)$  denotes the set of faces containing the vertices in  $A$ .

Let  $W = (w_0, w_1, w_2)$ ,  $w_i = (w_{ix}, w_{iy})$ ,  $i = 0, 1, 2$  be a triple of 2D points. When  $(w_0, w_1, w_2)$  do not lie on a line, they form a triangle. The directed area of the triangle is given by the determinant of  $W$ , which is defined by

$$\det(W) = \begin{vmatrix} 1 & 1 & 1 \\ w_{0x} & w_{1x} & w_{2x} \\ w_{0y} & w_{1y} & w_{2y} \end{vmatrix}. \quad (2.1)$$

When  $(w_0, w_1, w_2)$  are counter-clockwise oriented,  $\det(W) > 0$ ; otherwise,  $\det(W) < 0$ .

Let  $W = (w_0, w_1, w_2)$  and  $x$  be a triangle and a point in  $R^2$ . Then the barycentric coordinates  $(\lambda_0, \lambda_1, \lambda_2)$  of  $x$  with respect to  $W$  are

$$(\lambda_0(x|W), \lambda_1(x|W), \lambda_2(x|W)) = \frac{1}{\det(W)} (\det(x, w_1, w_2), \det(w_0, x, w_2), \det(w_0, w_1, x)). \quad (2.2)$$

The barycentric coordinates have properties:  $\lambda_0 + \lambda_1 + \lambda_2 = 1$  and  $\lambda_0 w_0 + \lambda_1 w_1 + \lambda_2 w_2 = x$ .

Given a knot set  $U = (t_0, \dots, t_{k+2})$  of size  $k+3$  in  $R^2$ , arbitrarily choose three knots  $(t_{i_0}, t_{i_1}, t_{i_2})$  from  $U$  that are not collinear and form a triangle  $W$ . A degree  $k$  bivariate simplex spline associated with  $U$  is a piecewise polynomial defined recursively by

$$M(x|U) = \sum_{j=0}^k \lambda_j(x|W) M(x|U \setminus \{t_{i_j}\}), \quad x \in R^2. \quad (2.3)$$

When  $k = 0, U = (t_0, t_1, t_2)$  and the degree 0 simplex spline is

$$M(x|\{t_0, t_1, t_2\}) = \frac{\chi[t_0, t_1, t_2](x)}{\det(t_0, t_1, t_2)}$$

where  $\chi[t_0, t_1, t_2](x)$  is the characteristic function on the triangle  $(t_0, t_1, t_2)$  [22]. Simplex splines possess many nice properties that univariate B-splines have. For example, simplex splines have a finite support that is the convex hull of knots  $U$ . If all knots in  $U$  are in generic positions, i.e., no three knots in  $U$  are linearly dependent, simplex splines are  $C^{k-1}$  continuous. If there are  $s$  collinear knots in  $U$ , the continuity will reduce to  $C^{k-s+1}$ , which is similar to the multiple knot case in univariate B-splines.

Some notations are given below:

- $[i]_j$  means  $i$  modulo  $j$ .
- $\text{conv}(S)$  denotes the convex hull of all points in  $S$ , which is a convex polygon with vertices in  $S$ . A point in  $S$  is an extreme point if it is a vertex of the convex hull of  $S$ .
- $\text{int}(T)$  denotes the interior of the region tessellated by a triangulation  $T$ .
- $\text{supp}(f)$  denotes the support of the function  $f$ .

### 3 BIVARIATE SPLINES ON 2D TRIANGULATION

In this section, we construct a bivariate spline space for a given triangulation using simplex splines. A spline function is defined over knots. Compared to univariate B-splines that are defined over a set of consecutive knots (numbers), it is much more difficult to specify knots (2D points) for bivariate splines over a triangulation domain. Therefore in the following we first propose some rules for knot selection in order to construct bivariate splines.

For a planar region  $D$  bounded by a polygon, if we order the vertices of the polygon such that they are in the counter-clockwise direction, they form a directed cycle of region  $D$ . We denote this directed cycle by  $C_R(D)$ . Now consider a triangulation  $T = \{V, E, F\}$  in  $R^2$ . We define a *degree  $k$  directed-one-ring cycle (DIRC) configuration* as  $X = (X_c, X_i)$  where  $X_i$  is an interior vertex set consisting of one vertex, two vertices of an edge, or three vertices of a face of  $T$  for  $k = 1, 2$  and  $3$ , respectively; and  $X_c$  is the directed one-ring-cycle of  $X_i$ . Specifically, when  $k = 1$ ,  $X_i$  contains only one interior vertex  $v$  of  $T$ , and then  $X_c = C_R\left(\bigcup_{f \in \Gamma^f(v)} f\right)$ . When  $k = 2$ ,  $X_i$  consists of two interior vertices  $v_1$  and  $v_2$  that form an edge in  $T$ ,

and  $X_c = C_R\left(\bigcup_{f \in \Gamma^f(v_1, v_2)} f\right)$ . When  $k = 3$ ,  $X_I$  consists of three interior vertices  $v_1, v_2$  and  $v_3$  that form a triangle in  $T$ , and  $X_c = C_R\left(\bigcup_{f \in \Gamma^f(v_1, v_2, v_3)} f\right)$ . With reference to Fig. 1, three D1RCs of degrees 1, 2 and 3 are shown from left to right. The knots in the interior vertex sets are colored red. The vertices of the directed-one-ring-cycles are displayed in blue and connected with dashed lines, where the arrows indicate the directions.

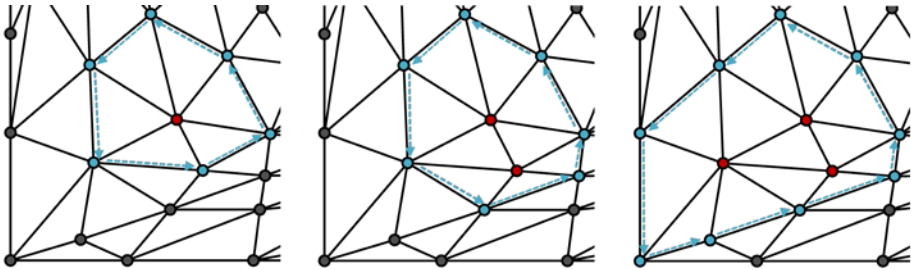


Fig. 1: From left to right: degree 1, 2 and 3 directed-one-ring cycle configurations. The interior vertex sets  $X_I$  are colored red, and the directed one-ring-cycles  $X_c$  are colored blue.

Let  $X = (X_c, X_I)$  be a degree  $k$  D1RC configuration. Assume  $X_c = (v_0, \dots, v_n)$ . A degree  $k$  D1RC-spline associated with  $X$  is defined as a combination of degree  $k-1$  simplex splines:

$$b_X^k(t) = \sum_{i=0}^n \det(v_i, v_{i+1}, t) M(t | X_I \cup \{v_i, v_{i+1}\}), \quad t \in R^2 \tag{3.1}$$

where  $\det(v_i, v_{i+1}, t)$  is the directed area of triangle  $(v_i, v_{i+1}, t)$ , and  $M(t | X_I \cup \{v_i, v_{i+1}\})$  is the simplex spline defined over the knot set  $X_I \cup \{v_i, v_{i+1}\}$ . Fig. 2 shows a degree 3 D1RC configuration (left) and its corresponding degree 3 D1RC-spline function (right).

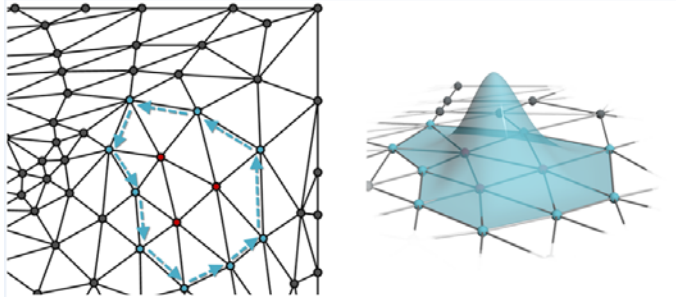


Fig. 2: A degree 3 D1RC configuration and its corresponding D1RC-spline.

Now we show that the constructed D1RC-splines have many nice properties as univariate B-splines. In fact, we have

**Proposition 1.** A degree  $k$  D1RC-spline is non-negative and  $C^{k-1}$  continuous if knots are in generic position, and has local support.

*Proof.* Let us first prove that the degree  $k$  D1RC-spline is a linear combination of degree  $k$  simplex splines. Recall that a degree  $k$  simplex spline can be represented as a combination of degree  $(k-1)$  ones. Hence when  $X_c$  contains three vertices, the situation becomes trivial. This is because  $b_X^k(t)$  defined in Eqn. (3.1) is the degree  $k$  simplex spline defined over knot set  $X_I \cup X_c$ .

Consider the situation where  $X_C$  is a quadrilateral  $(v_0, v_1, v_2, v_3)$ . We triangulate it into two triangles  $(v_0, v_1, v_3)$  and  $(v_1, v_2, v_3)$  by simply connecting diagonal  $v_1v_3$ . Now two degree  $k$  simplex splines can be defined over knot sets  $X_I \cup (v_0, v_1, v_3)$  and  $X_I \cup (v_1, v_2, v_3)$ , respectively. Let us consider the linear combination of the two simplex splines:

$$M^*(t) = \det(v_0, v_1, v_3)M(t | X_I \cup \{v_0, v_1, v_3\}) + \det(v_1, v_2, v_3)M(t | X_I \cup \{v_1, v_2, v_3\}). \quad (3.2)$$

Using the recurrence relation in Eqn. (2.3), Eqn. (3.2) can be rewritten as

$$\begin{aligned} M^*(t) &= \sum_{i=0}^3 \det(v_i, v_{[i+1]_4}, t)M(t | X_I \cup \{v_i, v_{[i+1]_4}\}) \\ &\quad + \det(v_1, v_3, t)M(t | X_I \cup \{v_1, v_3\}) + \det(v_3, v_1, t)M(t | X_I \cup \{v_1, v_3\}) \\ &= b_X^k(t). \end{aligned} \quad (3.3)$$

The second equality holds due to  $\det(v_1, v_3, t) = -\det(v_3, v_1, t)$ . Thus the degree  $k$  D1RC-spline can be expressed as a linear combination of degree  $k$  simple simplex splines with non-negative coefficients  $\det(v_0, v_1, v_3)$  and  $\det(v_1, v_2, v_3)$ . Moreover, it can be verified that  $M^*(t) \equiv b_X^k(t)$  of Eqn. (3.3) is independent of the choice of the diagonal of the quadrilateral. This is because each diagonal corresponds to a pair of oppositely directed edges whose contributions will cancel each other in the basis conversion.

When  $X_C$  forms a general simple polygon, we can similarly prove that a degree  $k$  D1RC-spline is a linear combination of degree  $k$  simplex splines. This is because the polygon can be triangulated into a set of triangles and adjacent triangles share a pair of oppositely directed edges.

Since degree  $k$  simplex splines have the properties of non-negativity,  $C^{k-1}$  continuity and local support, we can conclude that the degree  $k$  D1RC-spline has the same properties based on Eqn. (3.2) and Eqn. (3.3). Moreover, we have

$$\text{supp}(b_X^k(t)) = \bigcup_{i=0}^{n-1} \text{conv}(X_I \cup \{v_i, v_{(i+1)_n}\}) \text{ and } \bigcup_{f \in \{\Gamma^f(v) | v \in X_I\}} f \subseteq \text{supp}(b_X^k(t)) \subseteq \text{conv}(X_I \cup X_C).$$

This completes the proof. □

For a triangulation  $T = \{V, E, F\}$  in  $R^2$ , let  $X_T^k$  be the set of all possible degree  $k$  D1RC configurations. Then the set of degree  $k$  D1RC-splines  $\{b_X^k | X \in X_T^k\}$  forms a degree  $k$  spline space.

## 4 BIVARIATE SPLINE SURFACE MODELING

In classic B-spline curves and surfaces, a set of 3D points is used as the coefficients in the curve and surface formulation. These points are connected to form a polygon or mesh which gives the rough shape of the curves or surfaces. Meanwhile, they serve as control points providing an intuitive interface for users to design and manipulate the shape. In this section, we aim to develop a similar scheme for the proposed bivariate splines. Hence the input to our problem is a 3D triangular mesh topologically equivalent to a disk, which can be represented as  $T = \{V, E, F\}$  where  $V$  is a set of 3D vertices,  $E$  is a set of edges and  $F$  is a set of triangles. The goal is to construct a spline surface from  $T$  such that the vertices of  $T$  serve as the control vertices as in NURBS and the triangular mesh mimics the shape of the spline surface.

Our basic idea is to properly define bivariate spline functions proposed in previous section for the input triangular mesh, which exhibit many nice properties of univariate B-splines, and then use them to construct the blending functions for spline surface definition. Our method mainly consists of four steps outlined below:

- Parameterize the input triangular mesh

To define a parameter domain and knots for spline surfaces, we parameterize the input triangular mesh, which maps the triangular mesh to a triangulation on a 2D domain. For convenience, we denote the triangulation by  $T = \{V, E, F\}$  which are the images of  $T = \{V, E, F\}$ . There have been many parameterization methods such as conformal parameterization and

equiareal parameterization. In this paper, we use the mean value coordinates based parameterization method [12], which is a conformal parameterization and is often suggested because the one-to-one mapping is guaranteed when the domain boundary is convex. Fig. 3(e) shows an example of parameterization of the input triangular mesh given in Fig. 3(a).

- Construct D1RC configurations and D1RC-splines

Once we obtain the 2D triangulation  $T = \{V, E, F\}$ , we construct the set of all possible degree  $k$  D1RC configurations, which also define the set of degree  $k$  D1RC-splines.

- Construct the rational spline surface

We relate the degree  $k$  D1RC-splines to the input 3D triangular mesh, which then defines a rational spline surface. The input triangular mesh serves as a control grid for the surface.

- Model sharp features

Local D1RC configurations can be modified in order to model sharp features in the surface.

The details of the last two steps are further elaborated in the following subsections.

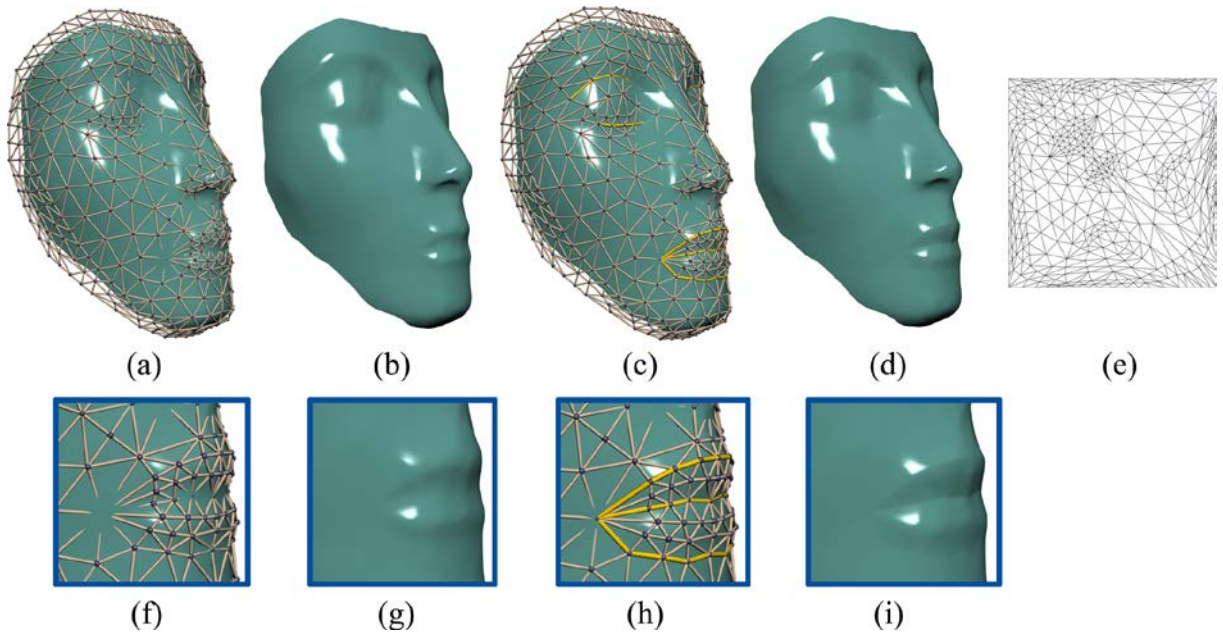


Fig. 3: Degree 3 D1RC-spline surfaces. (a) Input triangular mesh; (b) The D1RC-spline surface; (c) Specify sharp edges (in yellow) on the control mesh; (d) The resulting D1RC-spline surface with sharp features; (e) The parameterization of the input mesh in (a); (f)-(i) The close-up views of (a)-(d) in the areas of the mouth to compare the modeling of sharp features.

#### 4.1 Construction of Rational Spline Surfaces

Given an input 3D triangular mesh  $T = \{V, E, F\}$  and its corresponding 2D triangulation  $T = \{V, E, F\}$  on the parameter domain, we denote by  $X_T^k$  all the degree  $k$  D1RC configurations. For each element  $X = (X_c, X_l) \in X_T^k$ , its D1RC-spline is  $b_X^k$ . Denote by  $P_X$  the average of all the 3D vertices in  $X_l$  of the D1RC configuration  $X = (X_c, X_l)$ , i.e.,  $P_X = \frac{1}{k} \sum_{v_i \in X_l} v_i$ . Let  $\Omega = \text{conv}(V \cap \text{int}(T))$ . Then the D1RC-spline surface is defined as

$$P(t) = \frac{\sum_{X \in X_T^k} P_X b_X^k(t)}{\sum_{X \in X_T^k} b_X^k(t)}, \quad t \in \Omega. \quad (4.1)$$

Here the D1RC-splines are normalized to have the property of partition of unity, which ensures the convex hull property of the surface. We can also rewrite Eqn. (4.1) as

$$P(t) = \sum_{\mathbf{v}_i \in \mathbf{V}} \mathbf{v}_i B_i^k(t), \quad t \in \Omega \quad (4.2)$$

where  $B_i^k(t) = \frac{\sum_{X=(X_c, X_l), \mathbf{v}_i \in X_l} b_X^k(t)}{k \sum_{X \in X_l^k} b_X^k(t)}$  is a piecewise rational function, serving as a blending function for

vertex  $\mathbf{v}_i$ , and it has the same continuity as  $b_X^k(t)$ . Fig. 4 shows a triangular mesh that is placed on a plane. One vertex is pulled up from the plane and its corresponding blending functions of degrees 1, 2 and 3 are displayed from left to right.

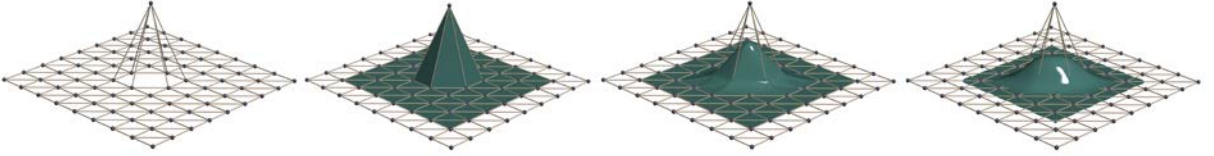


Fig. 4: Illustration of the blending function of degrees 1, 2 and 3 for one vertex that is pulled up from the plane.

It can be seen from Eqn. (4.2) that the D1RC-spline surface is defined as the sum of control points multiplied by blending functions, which is similar to NURBS. Obviously, the D1RC-spline surface has the properties of affine invariance, local control, etc. Fig. 3 (b) shows such a spline surface.

## 4.2 Modeling of Sharp Features

The surface defined by Eqn. (4.2) is  $C^{k-1}$  continuous in general. In order to introduce sharp features, we can use collinear knots which are an analog of multiple knots in univariate B-splines. In fact, if there are  $s$  collinear knots, the constructed spline is  $C^{k-s+1}$  continuous along the line. Upon this, we propose a special construction of D1RC configurations to achieve  $C^0$  continuity along a specified edge. Assume that an edge with vertices  $\mathbf{v}_1$  and  $\mathbf{v}_2$  are labelled as a sharp edge and their corresponding knots in  $R^2$  are  $\mathbf{v}_1$  and  $\mathbf{v}_2$ . We construct two degree  $k$  D1RC configurations  $(X_c^j, X_l^j)$  for  $j = 1, 2$ , with  $X_l^1 = \{\mathbf{v}_1 + \frac{s}{k}(\mathbf{v}_2 - \mathbf{v}_1) : s = 0, \dots, k-1\}$  and  $X_l^2 = \{\mathbf{v}_2 + \frac{s}{k}(\mathbf{v}_1 - \mathbf{v}_2) : s = 0, \dots, k-1\}$ . Hence there are  $k+1$  knots lying on the edge  $\mathbf{v}_1 \mathbf{v}_2$ , which result in  $C^0$  continuity. Refer to Fig. 5 for an example where a pair of degree 3 D1RC configurations is constructed. Fig. 3(c) shows that a few edges in the areas of the right eye and the mouse are labelled as sharp edges. With the special D1RC configurations, we can achieve the sharp features in the surface as shown in Fig. 3(d). The close-up views are given in Fig. 3(f-i).

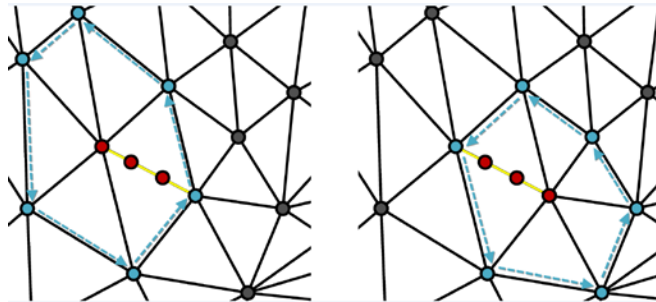


Fig. 5: Construction of degree 3 D1RC configurations for a sharp edge. The specified sharp edge is highlighted in yellow. The interior vertex set and the D1RCs are colored in red and blue, respectively.

## 5 EXPERIMENTS

This section presents some examples to demonstrate the capability of the proposed D1RC-spline surfaces. The models used in the experiments are initially dense meshes. We simplify them into coarse meshes which are then used as the input control meshes. The closed meshes are further converted to open meshes by removing some faces such that they are homeomorphic to a planar disk. To set up knots, we map the input control meshes onto a planar domain. For a given input control mesh, different choices of the parameter domain and parameterization may lead to different results. For the sake of simplicity, in our experiments we just choose the unit square as the parameter domain and the parameterization is performed by using CGAL package. After these steps, the bivariate spline surfaces are constructed.

Fig. 6 shows a triangular mesh with arbitrary connectivity, based on which three D1RC-spline surfaces are defined, corresponding to degrees 1, 2, and 3, respectively. It can be seen that the smoothness of the surfaces is improved when the degree of the surfaces increases. Fig. 7 shows an example where moving one vertex of the input triangular mesh locally adjusts the shape of the surface. This is because the blending function corresponding to the vertex has local support.



Fig. 6: D1RC-spline surfaces defined over the same input triangular mesh. From left to right: input triangular mesh, degree 1 surface, degree 2 surface, and degree 3 surface.

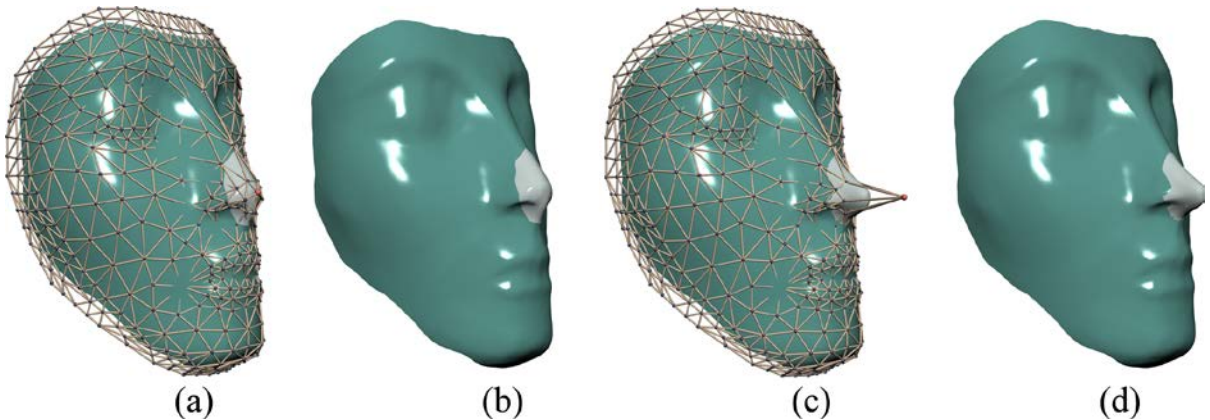


Fig. 7: The influence region of a control point in a degree 3 D1RC-spline surface. (a) The D1RC-spline surface and the control mesh, where the selected control point and his influence region are visualized in red and white, respectively; (b) The D1RC-spline surface; (c) The selected control point is moved and the shape of the surface is locally adjusted; (d) the adjusted surface.

Fig. 8 gives two degree 3 D1RC-spline surfaces for representing a screwdriver and a mask of Nicolò da Uzzano. Both models have uneven distribution of shape variations, which makes fitting using tensor-product B-splines inefficient. Relatively, the proposed bivariate spline surface modeling does not suffer from the tensor-product constraint and is thus more flexible. Fig. 9 demonstrates how to

introduce sharp features to enhance the quality of the surface. With the special D1RC configurations, the sharp features can be better modeled.



Fig. 8: Left: input mesh with 631 vertices and the resulting D1RC-spline surface; Right: input mesh with 1290 vertices and the resulting D1RC-spline surface.

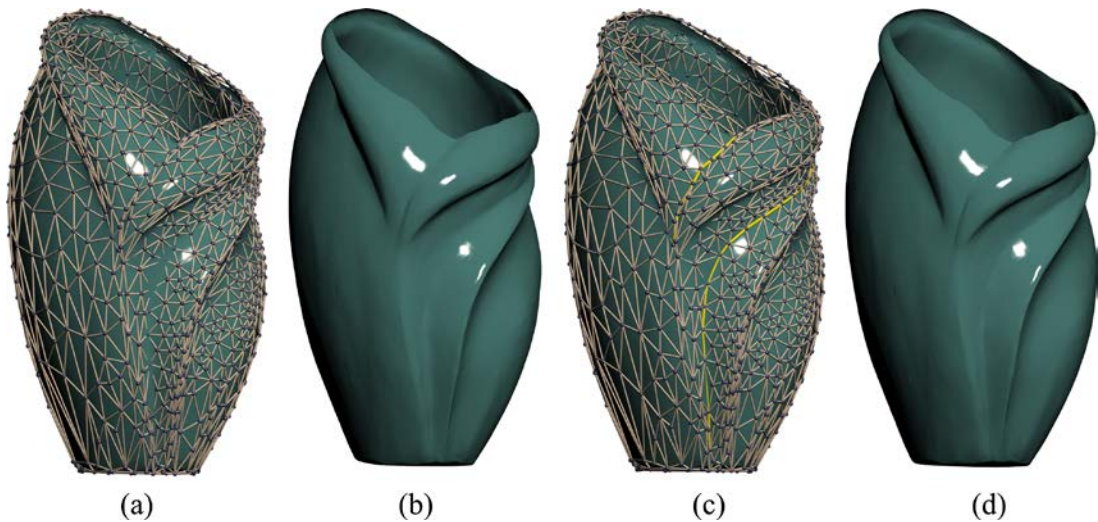


Fig. 9: (a) Input triangular mesh with 820 vertices; (b) Degree 3 D1RC-spline surface; (c) Some edges are labelled as a sharp edges (in yellow); (d) The resulting surface with  $C^0$  continuity along the feature lines corresponding to the labelled edges.

## 6 CONCLUSIONS

We have described a novel approach to generalizing univariate B-splines to bivariate splines defined on a 2D triangulation and then a scheme to define rational spline surfaces from 3D triangular meshes. The proposed scheme defines spline surfaces in a way similar to that of NURBS, but has less restriction on the connectivity of the input mesh, just as subdivision surfaces. Compared to existing non-tensor product spline schemes based on simplex splines, our approach has advantages. In particular, compared to DMS-splines, our method is free from specifying auxiliary knots. Compared to DCB-splines which are constructed based on the Delaunay configurations and have difficulty to construct

blending functions for the vertices of an input mesh, our method is more intuitive and does not require special triangulation. Our work provides a new way to construct bivariate splines on general triangular meshes and inspires further exploration.

Our current work has several limitations. First, this paper focuses on the construction of surfaces of degrees 1, 2 and 3. While it is possible to extend the idea to define surfaces of any degree, the extension with an intuitive construction is nontrivial. Second, though the proposed scheme produces  $C^{k-1}$  continuous surfaces, the fairness of the surfaces depends on the distribution of the vertices of the input mesh. How to place the control vertices properly to produce visually pleasing shapes is an interesting problem. Third, some fundamental issues, such as the influence of parameterization on the shape of the surface, degree elevation, refinement, and boundary control, are worth future investigation.

Juan Cao, <http://orcid.org/0000-0002-8154-4397>

Jianmin Zheng, <http://orcid.org/0000-0002-5062-6226>

## ACKNOWLEDGEMENTS

This work is supported by MOE AcRF Tier 1 Grant of Singapore (RG26/15), National Nature Science Foundation of China (No.61100106, No.61472332), the Natural Science Foundation of Fujian Province of China (No. 2015J01273) and the Fundamental Research Funds for the Central Universities (No.20720150002).

## REFERENCES

- [1] Beccari, C.; Gonsor, D.; Neamtu, M.: RAGS: Rational geometric splines for surfaces of arbitrary topology, *Computer Aided Geometric Design*, 31 (2), 2014, 97-110. <http://dx.doi.org/10.1016/j.cagd.2013.11.004>
- [2] Cao, J.; Li, X.; Chen, Z.; Qin, H.: Spherical DCB-spline surfaces with hierarchical and adaptive knot insertion, *IEEE Transactions on Visualization and Computer Graphics*, 18(8), 2012, 1290-1303. <http://dx.doi.org/10.1109/TVCG.2011.156>
- [3] Cao, J.; Li, X.; Wang, G.; Qin, H.: Surface reconstruction using bivariate simplex splines on Delaunay configurations, *Computers & Graphics*, 33(3), 2009, 341-350. <http://dx.doi.org/10.1016/j.cag.2009.03.013>
- [4] Catmull, E.; Clark, J.: Recursively generated B-spline surfaces on arbitrary topological meshes, *Computer-Aided Design*, 10(6), 1978, 350-355. [http://dx.doi.org/10.1016/0010-4485\(78\)90110-0](http://dx.doi.org/10.1016/0010-4485(78)90110-0)
- [5] Chen, Z.; Xiao, Y.; Cao, J.: Approximation by piecewise polynomials on Voronoi tessellation, *Graphics Models*, 76(5), 2014, 522-531. <http://dx.doi.org/10.1016/j.gmod.2014.04.006>
- [6] Dahmen, W.; Micchelli, C.; Seidel, H.P.: Blossoming begets b-spline bases built better by b-patches, *Mathematics of Computation*, 59, 1992, 97-115. <http://dx.doi.org/10.2307/2152982>
- [7] De Boor, C.: The way things were in multivariate splines: a personal view, in *Multiscale, Nonlinear and Adaptive Approximation*, 2009, 10-37. [http://dx.doi.org/10.1007/978-3-642-03413-8\\_2](http://dx.doi.org/10.1007/978-3-642-03413-8_2)
- [8] De Boor, C.; Höllig, K.; Riemenschneider, S.: *Box Splines*, Springer-Verlag New York, New York, USA, 1993. <http://dx.doi.org/10.1007/978-1-4757-2244-4>
- [9] Dembart, B.; Gonsor, D.; Neamtu, M.: Bivariate quadratic B-splines used as basis functions for data fitting, *Mathematics for Industry: Challenges and Frontiers 2003 (A Process View: Practice and Theory)*, 2005, 179-198.
- [10] Doo, D.; Sabin, M.: Behaviour of recursive division surfaces near extraordinary points, *Computer-Aided Design*, 10(6): 1978, 356-360. [http://dx.doi.org/10.1016/0010-4485\(78\)90111-2](http://dx.doi.org/10.1016/0010-4485(78)90111-2)
- [11] Farin, G.: Triangular Bernstein-Bézier patches, *Computer Aided Geometric Design*, 3(2), 1986, 83-127. [http://dx.doi.org/10.1016/0167-8396\(86\)90016-6](http://dx.doi.org/10.1016/0167-8396(86)90016-6)
- [12] Floater, M.: Mean value coordinates, *Computer Aided Geometric Design*, 20(1), 2003, 19-27. [http://dx.doi.org/10.1016/S0167-8396\(03\)00002-5](http://dx.doi.org/10.1016/S0167-8396(03)00002-5)
- [13] Franssen, M.: Evaluation of DMS-splines, Master's thesis, Eindhoven University of Technology, 1995.

- [14] Greiner, G.; Seidel, H.P.: Modeling with triangular B-splines, IEEE Computer Graphics and Applications, 14, 1993, 211-220. <http://dx.doi.org/10.1145/164360.164425>
- [15] Neamtu, M.: Bivariate simplex B-splines: a new paradigm, Proceedings of the 17th Spring Conference on Computer Graphics, Wahsington, DC, USA, 2001, 71-78, IEEE Computer Society. <http://dx.doi.org/10.1109/SCCG.2001.945339>
- [16] Neamtu, M.: What is the natural generalization of univariate splines to higher dimensions? Vanderbilt University, Nashville, TN, USA, 2001.
- [17] Piegl, L.; Tiller, W.: The NURBS Book, Springer-Verlag Berlin Heidelberg, 1997, ISBN 978-3-642-59223-2. <http://dx.doi.org/10.1007/978-3-642-59223-2>
- [18] Pfeifle, R.; Seidel, H.: Spherical triangular B-splines with application to data fitting, Computer Graphics Forum, 14(3), 1995, 89-96. <http://dx.doi.org/10.1111/1467-8659.1430089>
- [19] Sederberg, T.W.; Cardon, D.L.; Finnigan, G.T.; North, J.; Zheng, J.; Lyche, T.: T-spline simplification and local refinement, ACM Transactions on Graphics, 23, 2004, 276-283. <http://dx.doi.org/10.1145/1015706.1015715>
- [20] Sederberg, T.W.; Zheng, J.; Bakenov, A.; Nasri, A.: T-splines and T-NURCCs, ACM Transactions on Graphics, 22, 2003, 477-484. <http://dx.doi.org/10.1145/882262.882295>
- [21] Sederberg, T.W.; Zheng, J.; Sewell, D.; Sabin, M.: Non-uniform recursive subdivision surfaces, Proceeding of ACM SIGGRAPH 1998, Orlando, USA. <http://dx.doi.org/10.1145/280814.280942>
- [22] Seidel, H.P.: Polar forms and triangular B-spline surfaces, in Blossoming: The New Polar-Form Approach to Spline Curves and Surfaces, SIGGRAPH'91 Course Notes 26, World Scientific Publishing Co, 1992, 235-286. [http://dx.doi.org/10.1142/9789814355858\\_0007](http://dx.doi.org/10.1142/9789814355858_0007)